Interfacial exchange coupling in Fe-Tb/[Co/Pt] heterostructures

C. Schubert,[1] B. Hebler,[1] H. Schletter,[1] A. Liebig,[1] M. Daniel,[1] R. Abrudan,[2,3] F. Radu,[2] and M. Albrecht[1]

[1]*Institut für Physik, Technische Universität Chemnitz, Reichenhainer Straße 70, D-09126 Chemnitz, Germany*

[2]*Institut für Komplexe Magnetische Materialien, Helmholtz-Zentrum Berlin für Materialien und Energie, Albert-Einstein-Str. 15, 12489 Berlin, Germany*

[3]*Institut für Experimentalphysik/Festkörperphysik, Ruhr-Universität Bochum, Universitätsstraße 150, D-44780 Bochum, Germany*

(Received 13 September 2012; published 13 February 2013)

The exchange interaction and magnetization reversal processes in exchange-biased heterostructures consisting of amorphous ferrimagnetic Fe-Tb alloy films and ferromagnetic Co/Pt multilayers were investigated. Both film systems exhibit an easy axis magnetization perpendicular to the film plane. The dependence of the interfacial exchange coupling on the stoichiometry of the Fe-Tb layer as well as the number of repetitions in the Co/Pt multilayers were analyzed. The net magnetization and effective magnetic anisotropy of the Fe-Tb alloy films have an influence on the exchange energy per unit area. A large exchange-bias field up to 8 kOe is found to be accompanied by an interfacial domain wall as probed by element specific x-ray magnetic circular dichroism absorption measurements. This domain wall exhibits a total thickness between 3 and 4 nm and affects strongly the magnetization reversal in the heterostructure. Furthermore, a linear relation between the thickness of the ferromagnetic Co/Pt multilayers and the exchange-bias field is observed and can be attributed to a change of the location where the interfacial domain wall nucleates in the heterostructure.

DOI: 10.1103/PhysRevB.87.054415 PACS number(s): 71.70.Gm, 75.60.Jk, 75.70.Cn, 75.30.Gw

I. INTRODUCTION

In its common way the exchange-bias (EB) effect appears in ferromagnetic/antiferromagnetic (FM/AFM) bilayers, if the antiferromagnet is cooled below its blocking temperature in the presence of an external magnetic field and an exchange field produced by the magnetic moments of the ferromagnet as originally found in CoO/Co nanoparticles by Meiklejohn and Bean in 1956.[1] Generally, one considers the frozen or pinned uncompensated spins at the interface of the antiferromagnet as reason for the biasing effect.[2–4] However, this explanation loses its validity in ferrimagnetic/ferromagnetic (FI/FM) and FI/FI bilayer systems, which can also possess an exchange anisotropy.[5–7] Especially heterostructures with perpendicular magnetic anisotropy (PMA), in which a FI amorphous rare-earth–transition-metal alloy like Fe-Tb is in the proximity of a transition-metal magnet, exhibit peculiar coupling interactions at the interface.[8,9] The magnetic coupling in such systems consists of two types of pair interactions, an antiparallel exchange between the rare-earth (RE) and transition-metal (TM) moments and a parallel exchange of the TM moments themselves.[10] Therefore, the EB effect can arise by both interactions simultaneously and occurs even for fully compensated interfaces [Fig. 1(a)].

In this paper we investigate the interfacial exchange interaction between Fe-Tb alloy films and Co/Pt multilayers by varying the Tb content of the Fe-Tb layer and the number of bilayers in the Co/Pt multilayer stack.

II. EXPERIMENTAL DETAILS

Exchange coupled heterostructures with PMA consisting of amorphous FI Fe-Tb alloy films and FM Co/Pt multilayers were prepared at room temperature (RT) using magnetron (co-)sputtering from elemental targets in a UHV chamber. For all depositions the base pressure remained below 5×10^{-9} mbar and the Ar pressure was kept constant at 1.5×10^{-3} mbar. Beside standard Si(001) wafers with a 100-nm-thick thermally oxidized SiO_2 layer, 200-nm-thick Si_3N_4 membranes were used as substrates allowing x-ray magnetic circular dichroism (XMCD) absorption measurements in transmission geometry.

In the different series of samples the atomic stoichiometry of the Fe-Tb alloy film and the number of bilayers of the Co/Pt multilayers were varied probing their influence on the interfacial exchange coupling. The composition of the Fe-Tb alloy films was determined by Rutherford backscattering spectrometry (RBS) giving an accuracy of 1.0 at.%. Transmission Electron Microscopy (TEM) imaging and diffraction revealed that all Fe-Tb films exhibit an amorphous structure in the composition range from 14 to 30 at.% of Tb. Cross-section micrographs used to study the morphology of the interface between the two magnetic layers in the different sets of samples reveal interfacial roughness and intermixing within the range 1–2 nm, as seen in the TEM image taken from a $Fe_{81}Tb_{19}$(20 nm)/[Co(0.4 nm)/Pt(0.8 nm)]$_{10}$ heterostructure (Fig. 2).

The samples' integral magnetic properties were determined using a superconducting quantum interference device-vibrating sample magnetometer (SQUID-VSM). Hysteresis loops were taken with a maximum external field of ± 70 kOe in a temperature range 4–400 K. In order to analyze the magnetic sublattice configuration during the reversal process in the FI/FM layer stacks, XMCD absorption measurements were performed at the Fe L_3 edge (708 eV), Co L_3 edge (778 eV), and Tb M_5 edge (1241 eV) using the ALICE diffractometer installed at the PM3 beamline of Helmholtz-Zentrum Berlin (HZB). Element specific hysteresis loops were measured with a maximum external field of ± 7 kOe in a temperature range 10–300 K.

III. RESULTS AND DISCUSSION

A. Amorphous FI Fe-Tb alloy films

The FI structure of amorphous Fe-Tb alloy films is based on a negative exchange coupling between the 3*d* spin moment of

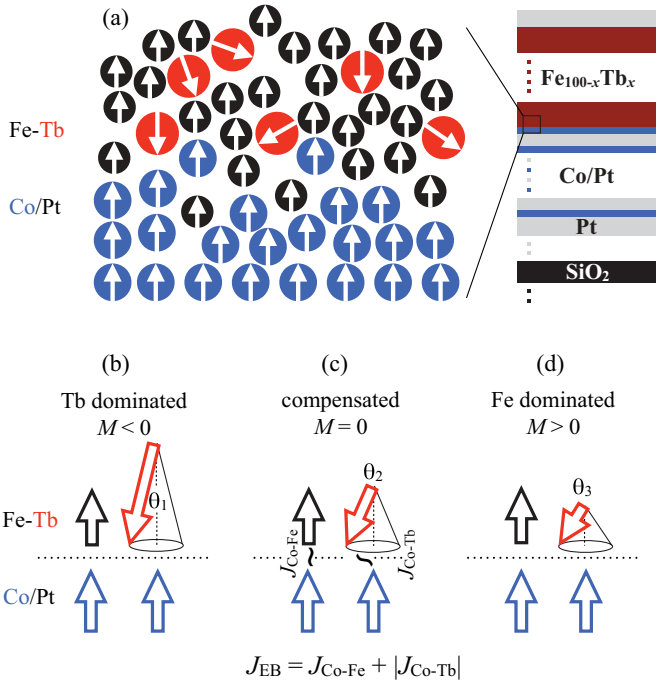

FIG. 1. (Color online) (a) General schematic view of the magnetic configuration in heterostructures with PMA consisting of FI amorphous Fe-Tb alloy films and FM Co/Pt multilayers. The black and the blue arrows represent the collinear alignment of the Fe and Co sublattices, respectively. In addition a drawing of a sample layer stack is given on the right. The red arrows with different length and opening angles θ illustrate the magnetic moment of the Tb sublattices and their average orientational distribution depending on the composition. (b)–(d) Average magnetic configuration illustrated by macrospins depending on the composition of the Fe-Tb alloy film. The opening angles $\theta_{1...3}$ of the Tb macro spins refer to the different fanning cone structures of the Tb sublattice. (b) The net magnetization of the Fe-Tb alloy film is dominated by the Tb sublattice. (c) The magnetic sublattices of the Fe and the Tb compensate each other and the net magnetization is zero. (d) The net magnetization of the Fe-Tb alloy film is dominated by the Fe sublattice. Please note that the different states depend on the Tb content and temperature.

the transition-metal electrons and the total magnetic moment (spin and angular moment) of the rare-earth $4f$ orbital.[10] In the composition range between 14 at.% and 30 at.% Tb, the alloy system can be classified with respect to the dominant magnetic moment influencing the existence of a magnetization compensation point in the temperature range up to the Curie temperature (T_C), which is about 400 K.[11] This behavior can be seen in the temperature dependence of the out-of-plane remanence magnetization for 20-nm-thick $Fe_{100-x}Tb_x$ single layers with different composition (Fig. 3). They serve also as reference samples for the heterostructures. The remanent magnetization was measured from 4 to 400 K after saturating the samples in an external magnetic field of 70 kOe at RT. Please note that the superconducting magnet of the SQUID-VSM was reset by heating over its transition temperature before the measurements to avoid the influence of an external remanent magnetic field.

$Fe_{100-x}Tb_x$ alloy films with $x \leqslant 20$ at.% reveal no magnetization compensation point. The net magnetization

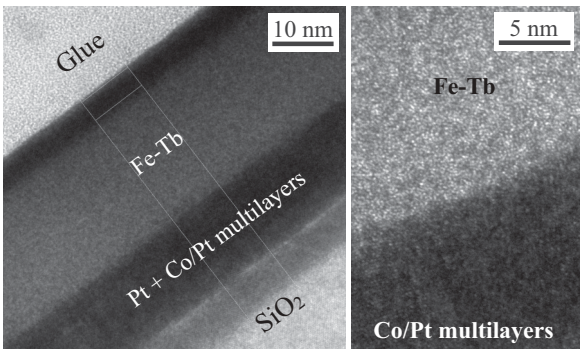

FIG. 2. TEM images with two different magnifications obtained in cross section geometry of a $Fe_{81}Tb_{19}$(20 nm)/[Co(0.4 nm)/Pt(0.8 nm)]$_{10}$ heterostructure embedded in Pt seed and capping layers revealing some roughness and intermixing at the Fe-Tb/[Co/Pt] interface.

is dominated by the Fe sublattice. In a composition range $20 < x \leqslant 24$ at.% the Fe-Tb alloys show a change of the dominant moment from Tb to Fe with increasing temperature. This is indicated by the net magnetization passing zero at the magnetization compensation temperature (T_{comp}). For the alloys with a Tb content of $x > 24$ at.%, the Tb sublattice becomes dominant in the whole temperature range. This agrees well with results presented in the literature.[11] However, please note that the specified composition regions depend on the preparation method and the type of seed layers because the growth mechanism has a strong influence on the magnetic anisotropy as well as the orientational distribution of the Tb moments due to the sperimagnetic nature of the amorphous Fe-Tb alloy system.[12,13]

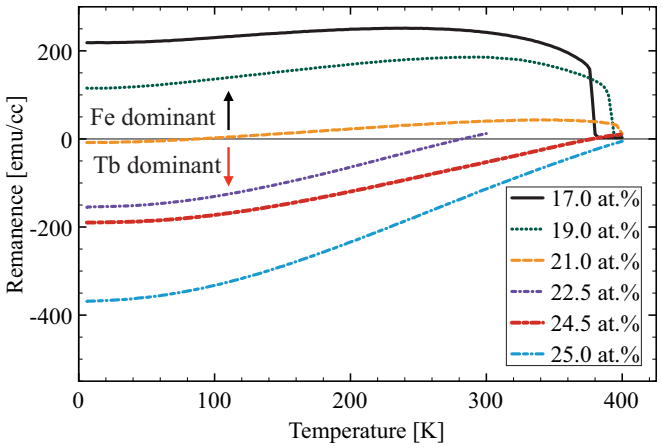

FIG. 3. (Color online) Out-of-plane remanence net magnetization as a function of the temperature and the composition obtained from 20-nm-thick $Fe_{100-x}Tb_x$ single layers used as reference samples for the heterostructures. The remanence magnetization was measured from 4 to 400 K after saturating the samples in an external magnetic field of 70 kOe at RT. The superconducting magnet of the SQUID VSM was reset by heating over its transition temperature before the measurement to avoid the influence of a small magnetic field coming from the remanence of the magnet. The positive and negative region of the net magnetization refers to a dominant Fe and Tb sublattice, respectively.

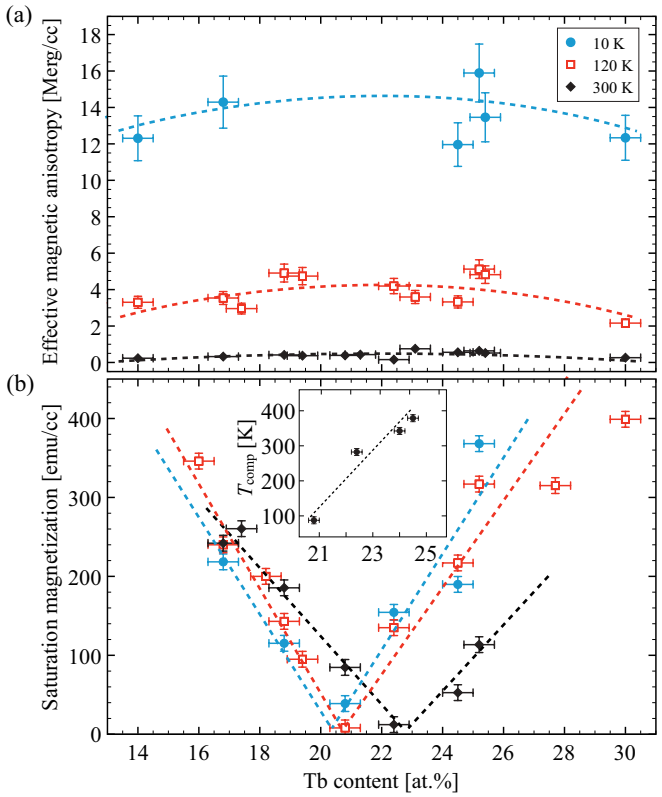

FIG. 4. (Color online) (a) The effective magnetic anisotropy and (b) the saturation magnetization of 20-nm-thick $Fe_{100-x}Tb_x$ alloy films as a function of the Tb content for various temperatures. These single layers serve as reference samples. The dashed curves act as a guide to the eye. The inset reveals the composition dependence of the compensation temperature.

The effective magnetic anisotropy (K_{eff}), which was calculated by coercivity and net magnetization[14] as a lower estimate, reveals also a strong temperature dependence, while the Tb content of the alloy has a rather weak impact, which can be seen in Fig. 4(a). Towards lower temperatures K_{eff} reaches values between 2 and 14 Merg/cc being relatively constant with respect to the alloy composition except for high and low amounts of Tb, where K_{eff} tends to decrease. The stoichiometry itself determines exclusively the net magnetization drawn in Fig. 4(b). Starting from the RT (300 K) compensation composition, the net magnetization increases from zero towards lower and higher amounts of Tb. Thus the magnetization compensation point depends strongly on the Tb content revealing a compensation temperature between 100 and 300 K for a Tb content between 20 and 24 at.%, respectively, as presented in the inset of Fig. 4(b).

In general, one assumes that the observed temperature dependence of K_{eff} and the net magnetization is attributed to the sperimagnetic nature of the amorphous Fe-Tb alloy system.[12–14] The Tb atoms possess a magnetic moment of about $9\mu_B$, which is hardly changing with temperature.[14] However, the magnetic configuration in such a thin alloy film exhibits an orientational distribution of the magnetic moments, which determines the total magnetization of the Tb sublattice. This noncollinearity results from the equilibrium between the exchange interaction of the Fe-Fe, Fe-Tb, and Tb-Tb pairs and the single-ion anisotropy of the Tb atoms caused by the interplay of their $4f$ orbitals with the local crystal field in the amorphous alloy.[15] Since the orientational distribution of the Tb moments varies with the temperature also K_{eff} and the net magnetization changes.

As their magnetic properties are easy to tune by varying the temperature or composition, amorphous Fe-Tb alloy films represent a model system to investigate the interfacial exchange coupling of FI/FM heterostructures with PMA.

B. Interfacial exchange coupling with regard to the dominant moment in the Fe-Tb alloy system

Similar to the intrinsic behavior of the Fe-Tb alloy system, the interfacial exchange interaction between Fe-Tb films and Co/Pt multilayers manifests itself in a parallel alignment of the Co and Fe moments and an antiparallel alignment of the Co and Tb moments (Fig. 1).[18] Varying the stoichiometry of the Fe-Tb alloy films across the magnetization compensation point, the dominant exchange coupling at the interface will change from FM to AFM. This is expected to influence the magnetization reversal of the whole heterostructure. To elucidate this, a series of Pt(3 nm)/$Fe_{100-x}Tb_x$(20 nm)/[Co(0.4 nm)/Pt(0.8 nm)]$_{10}$/Pt(4.2 nm)/substrate samples with a Tb content x varying from 16 to 25 at.% was prepared.

1. *Interfacial exchange coupling in Fe dominated heterostructures*

In Fig. 5(a) the magnetization reversal of $Fe_{81}Tb_{19}$(20 nm)/[Co(0.4 nm)/Pt(0.8 nm)]$_{10}$ heterostructures obtained from SQUID-VSM measurements along the out-of-plane direction at different temperatures is shown. The reversal behavior of this bilayer system is dominated by a FM exchange coupling between Fe and Co at the interface. Around RT both layers reverse simultaneously in a single process. With decreasing temperature the switching field of the Fe-Tb layer increases much stronger as compared to the Co/Pt multilayers. This leads to a two-step reversal of the magnetization (*e.g.*, at 70 and 140 K). The separate switching fields of both layers allows the unidirectional anisotropy to be revealed through a shift of the hysteresis loop of the Co/Pt multilayers. This occurs as soon as the switching field of the Fe-Tb layer becomes larger than the maximum applied external field. In particular, using a maximum external field of 70 kOe, the unidirectional anisotropy sets in at a temperature of 40 K, leading to a loop shift with an EB field of $H_{EB} \approx -4$ kOe.

An overview of the switching fields of the Fe-Tb layer ($H_{S,Fe\text{-}Tb}$) and the Co/Pt multilayers ($H_{S,Co/Pt}$) as a function of temperature as compared to K_{eff} of the single reference layers is given in Fig. 5(b). Please note that the switching field was estimated from the derivative of the magnetization curve in the reversal region using the peak center of a Gaussian fit function. In the temperature range from RT down to about 180 K the anisotropies of both layers are more or less the same leading to the observed simultaneous switching [Fig. 5(a), *e.g.*, at 300 K]. Furthermore, the sharp switching of the hysteresis loops indicates a magnetization reversal driven by domain-wall nucleation and propagation, which is possible due to the strong exchange coupling of the Co and Fe sublattices at the interface. The region below 180 K is characterized by a strong

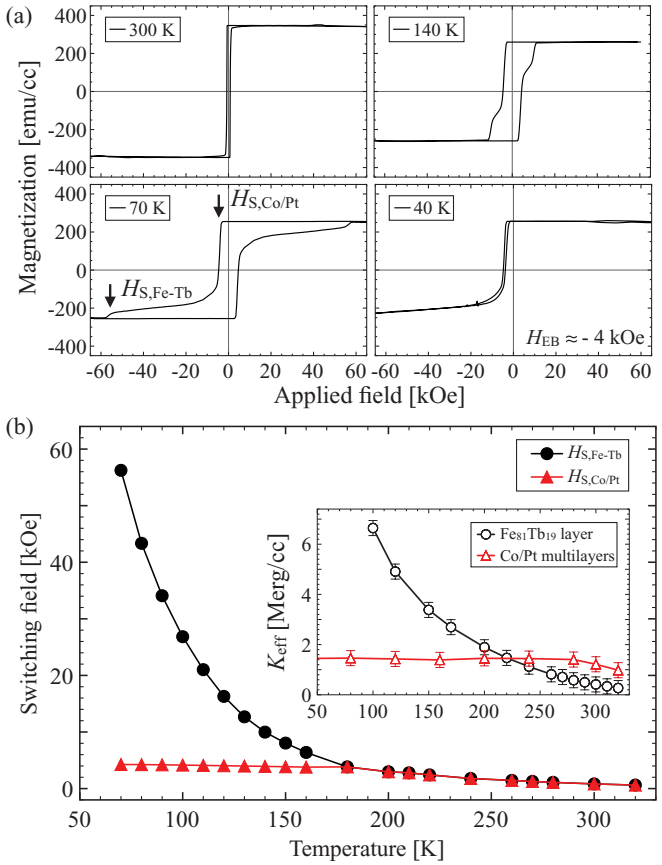

FIG. 5. (Color online) (a) Hysteresis loops of $Fe_{81}Tb_{19}$(20 nm)/[Co(0.4 nm)/Pt(0.8 nm)]$_{10}$ heterostructures measured in out-of-plane geometry at different temperatures using a SQUID-VSM and (b) switching field of the Fe-Tb layer ($H_{S,Fe-Tb}$) and the Co/Pt multilayers ($H_{S,Co/Pt}$) taken from the right branch of the hysteresis loop as a function of the temperature compared to the temperature dependence of K_{eff} of the single reference layers (inset).

enhancement of the Fe-Tb switching field having its origin in the increase of the magnetic anisotropy and the decrease of the net magnetization with decreasing temperature (Fig. 3).

In exchange coupled heterostructures the reversal of one layer against the other will produce an interfacial domain wall (IDW) in order to minimize the cost of energy for the magnetic transition region between both layers.[16] Referring to our system, with increasing external magnetic field the switching of the Co/Pt multilayers against the Fe-Tb alloy film occurs together with the formation of an IDW since in its ground state the Co and Fe sublattices prefer a parallel alignment, while the Tb sublattice favors pointing antiparallel to them. If now the external field will be reduced coming from this AFM configuration, at a certain field the IDW vanishes forcing the Co/Pt multilayers to rotate back so that the system can relax in its ground state. Due to the strong interfacial exchange coupling, the high amount of energy stored in the IDW gives rise to the large loop shift observed in this system.

The minor loop reversal study presented in Fig. 6 provides potential evidence for the occurrence of an IDW in the AFM configuration of the Fe-Tb alloy film and the Co/Pt multilayer. Starting from the remanent state after saturation, where the dominant moments of Fe and Co are aligned parallel as

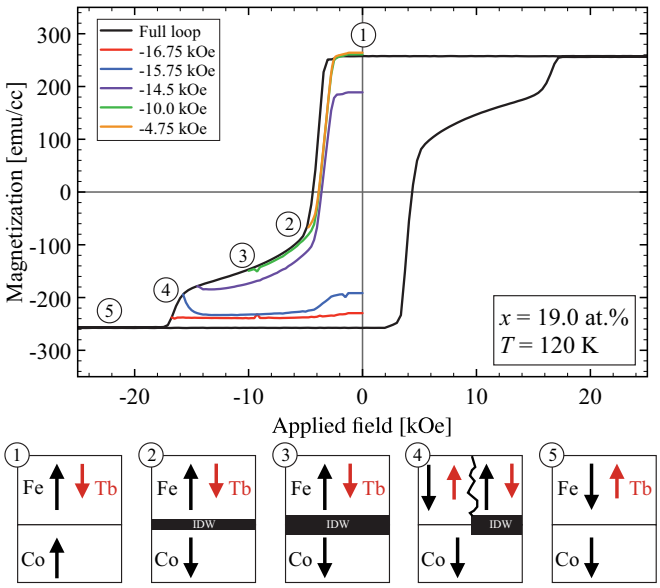

FIG. 6. (Color online) Minor loop reversal taken from out-of-plane SQUID-VSM measurements and a schematic drawing of the assumed domain configuration during the magnetization reversal in $Fe_{81}Tb_{19}$(20 nm)/[Co(0.4 nm)/Pt(0.8 nm)]$_{10}$ heterostructures.

illustrated by scheme number 1, an out-of-plane external field starts switching the Co/Pt multilayer leading to the formation of an IDW (scheme number 2). This behavior is completely reversible since the magnetization ends up in the same remanent state after reducing the field to zero. Even though the reversal field is increased further, as long as the switching field of the Fe-Tb layer is not reached, the reversal mechanism does not change. With regard to this, one can assume that the reversible characteristic is driven by nucleation and annihilation of the IDW during the field cycling. Furthermore, the reversibility in the higher field range can be attributed to an increasing or decreasing wall thickness depending on the applied field (see scheme number 3). Going on from cartoon 3 to 4 in the hysteresis loop, the increasing field starts to overcome the switching field of the Fe-Tb layer. In this intermediate state, where the Fe-Tb is not completely reversed, a partial shift of the minor loops still exists. This indicates that the reversal of the Fe-Tb layer is driven by the nucleation and expansion of lateral domains. These domains appear most likely as bubbles or stripes, which will not vanish in zero field.[17] This produces the configuration shown in the cartoon 4 of Fig. 6, in which some part of the heterostructure still possesses an IDW giving rise to the partially shifted minor loops observed when the field is reduced to zero. In particular, the minor loop produced by a reversal field of −15.75 kOe shows an unusual behavior, since the magnetization drops even more after reducing the external field. This might have its origin in a peculiar domain expansion during the reversal of the Fe-Tb layer. Finally, a further enhancement of the external field ends up in a complete reversal of the Fe-Tb layer modifying the remanent state (see cartoon number 5) since the IDW vanishes at saturation.

A confirmation of these findings is given by element specific XMCD absorption measurements performed for the $Fe_{83}Tb_{17}$(20 nm)/[Co(0.4 nm)/Pt(0.8 nm)]$_{10}$ heterostructure.

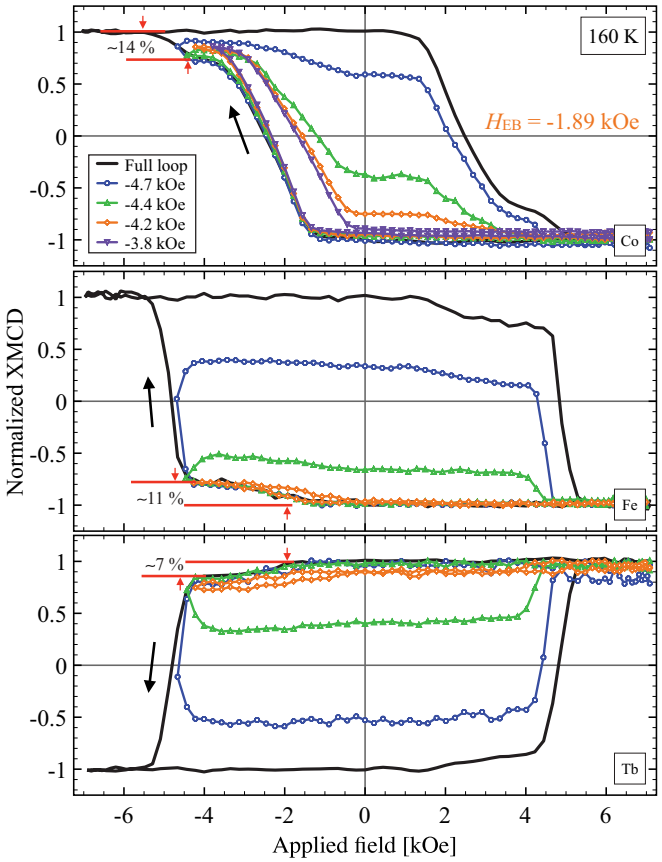

FIG. 7. (Color online) Element specific full and minor hysteresis loops of $Fe_{83}Tb_{17}$(20 nm)/[Co(0.4 nm)/Pt(0.8 nm)]$_{10}$ heterostructures obtained from XMCD absorption measurements at the L_3 edge of Fe (708 eV) and Co (778 eV) and the M_5 edge of Tb (1241 eV) of 160 K. The percentages indicate the portion of the XMCD signal related to the IDW.

The minor and full hysteresis loops of the Co, Fe, and Tb moments during the field cycling at a temperature of 160 K are shown in Fig. 7. From the full hysteresis loops one can find that the sign of the normalized XMCD signal changes for the Tb moments as compared to the Fe and Co moments referring to the antiparallel alignment between the rare-earth and transition-metal sublattices.[10] In addition, a small shoulder occurs in the hysteresis loops of the Fe and Tb moments during the reversal of the Co moments and *vice versa*. These features can be attributed to the proposed formation of an IDW, because the nucleation of such a domain wall will reduce the XMCD signal, which is proportional to the out-of-plane component of the magnetic moment. The portion of the shoulder as compared to the whole signal amounts to about 14% for Co, 11% for Fe, and 7% for Tb, which can be used to estimate the element specific portion of the domain-wall width t_{IDW}. Please note that the difference in the percentages between the Tb and Fe signals is caused most likely by the non-colinearity (fanning cone structure) of the Tb moments contributing less to the decrease in the signal by the nucleation of the IDW. Taking into account the Co and Fe percentages together with the thickness of the Co/Pt multilayers ($t_{Co/Pt} = 12$ nm) and the Fe-Tb layer ($t_{Fe\text{-}Tb} = 20$ nm) one can estimate the total domain wall width to $t_{IDW} = t_{IDW,Co/Pt} + t_{IDW,Fe\text{-}Tb} = (3.8 \pm 0.3)$ nm. Assuming that the IDW exhibits a structure similar to an ultrathin Néel wall, it is possible to determine the effective exchange stiffness A_{eff} of the material in the interface region using the following equation:[18]

$$A_{eff} = \frac{t_{IDW}^2}{4} K_{eff}. \quad (1)$$

With an effective anisotropy calculated from the values $K_{eff,Co/Pt} = (1.4 \pm 0.3)$ Merg/cm^3 for the Co/Pt multilayers and $K_{eff,Fe\text{-}Tb} = (2.3 \pm 0.4)$ Merg/cm^3 for the Fe-Tb alloy film as obtained from the reference samples at 160 K weighted by the thickness of the IDW ranging into each layer, the effective stiffness at the interface results in $A_{eff} = (6.8 \pm 2.6) \times 10^{-8}$ ergs/cm. In comparison to literature values[19,20] for Fe-Tb alloy films (1×10^{-7} ergs/cm) and Co/Pt multilayers (5×10^{-7} ergs/cm), the effective exchange stiffness is reduced at the interface. A reason for this can be the formation of a mixed layer at the Fe-Tb/[Co/Pt] interface.

Based on this result, one can recalculate the EB field via the energy density of the IDW, σ_{IDW}, using the following relations:[16,18,21–23]

$$H_{EB} = -\frac{J_{EB}}{M_S t} = -\frac{\sigma_{IDW}}{2M_S t}, \quad (2)$$

$$\sigma_{IDW} = 2\pi\sqrt{A_{eff} K_{eff}} = \pi t_{IDW} K_{eff}, \quad (3)$$

where J_{EB}, M_S, and t represent the interfacial exchange energy density, the saturation magnetization, and the thickness of the biased FM layer, respectively. According to the estimated domain-wall energy density of $\sigma_{IDW} = (2.2 \pm 0.7)$ ergs/cm^2, by using the measured values for t_{IDW} and K_{eff}, the EB field results to $H_{EB} = -(1.4 \pm 0.6)$ kOe. Please note that the specified error values were assessed by assuming a reduced anisotropy value at the interface according to the observed effective exchange stiffness. In comparison to the measured EB field of -1.89 kOe (see Fig. 7) the value estimated by the IDW model is in good agreement. For the calculations the magnetostatic interaction was not taken into account since only a marginal effect on the EB field due to the reduced magnetization of the Fe-Tb layer is expected, which will be discussed in more detail later. Calculations using the model of Meiklejohn and Bean[1] with the assumption of a close-packed structure of the atoms in the Fe-Tb alloy film lead to an almost ten times higher value. This can be seen as the maximum possible EB field for the material system appearing if the system would not develop an IDW in order to minimize the total energy.

2. *Interfacial exchange coupling in Tb dominated heterostructures*

With regard to the AFM exchange coupling between rare-earth and transition-metal moments, the magnetic configuration of the dominant moments in heterostructures consisting of Fe-Tb films and Co/Pt multilayers changes from FM to AFM with an increasing amount of Tb in the amorphous alloy film. This behavior is due to the fact that the net magnetization in amorphous Fe-Tb alloy films becomes dominated by the Tb moment when the Tb content is greater than 24 at.% (Fig. 3). In this section we will present an investigation on the interfacial exchange coupling in heterostructures exhibiting an AFM

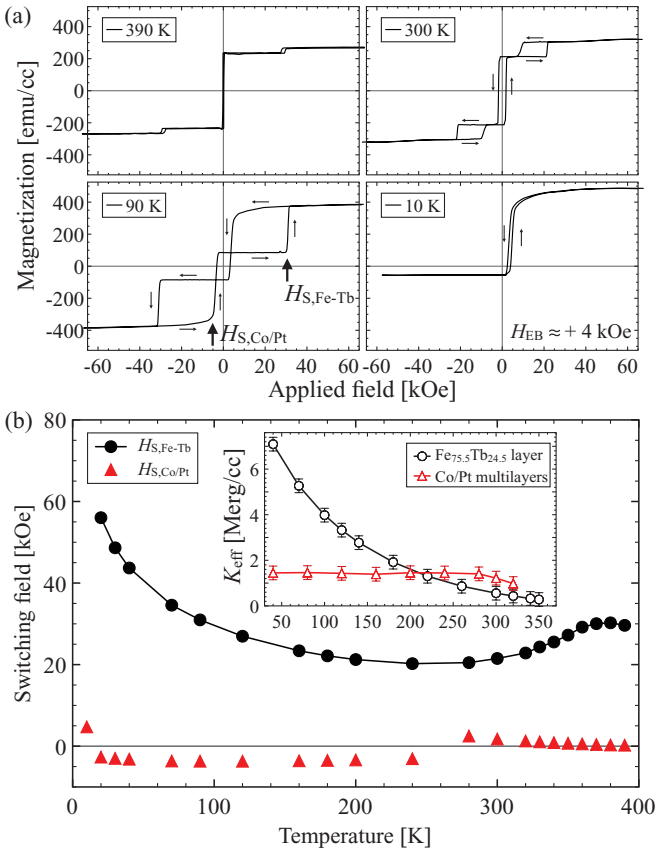

FIG. 8. (Color online) (a) Hysteresis loops of $Fe_{75.5}Tb_{24.5}$(20 nm)/[Co(0.4 nm)/Pt(0.8 nm)]$_{10}$ heterostructures measured in out-of-plane geometry at different temperatures using a SQUID VSM and (b) switching field of the Fe-Tb layer ($H_{S,Fe\text{-}Tb}$) and the Co/Pt multilayers ($H_{S,Co/Pt}$) as a function of temperature compared to the temperature dependence of K_{eff} of the single reference layers (inset). Please note that the increase in the switching field towards higher temperatures is related to the compensation point of the Fe-Tb layer, which is close to the Curie temperature.

configuration of the dominant moments. As a representative example, we will focus on the magnetization reversal behavior of the $Fe_{75.5}Tb_{24.5}$(20 nm)/[Co(0.4 nm)/Pt(0.8 nm)]$_{10}$ heterostructure.

The out-of-plane hysteresis loops in Fig. 8(a) give an overview of the magnetization reversal of the chosen bilayer system at different temperatures. In contrast to the simultaneous reversal in the Fe dominated heterostructures, as described in the prior section, one obtains a separate switching of the magnetic layers already at RT. Thereby, the Fe-Tb layer manifests its reversal in the appearance of satellite hysteresis loops at higher magnetic fields. This behavior can be attributed to a dominant AFM exchange coupling between the two layers and the nucleation of an IDW formed if the magnetization of both layers is aligned parallel to each other. With increasing temperature (*e.g.*, at 390 K) the observed satellite hysteresis loops do not vanish but become smaller, which is associated to the lowering of the saturation magnetization in the vicinity of T_C. Concerning the magnetization reversal of the Co/Pt multilayers, one observes an enhanced coercive field. In contrast to this behavior at lower temperatures (*e.g.*, at 90 K) the heterostructure relaxes after saturation in a positive field into its AFM remanent state by reversing the magnetization of the Co/Pt multilayers instead of the Fe-Tb film. This leads to the onset of a positive EB field $H_{EB,Co/Pt} \approx +4$ kOe of the Co/Pt multilayers, if the switching field of the Fe-Tb layer becomes larger than the external field (*e.g.*, at 10 K). A similar observation was made for in-plane FM/AFM and FI/FI systems with AFM interface coupling.[24,25]

An explanation for the observed reversal characteristic of the heterostructure can be deduced from the temperature dependence of the switching fields of the Fe-Tb layer and the Co/Pt multilayers compared to their effective magnetic anisotropy obtained from the single reference layers [inset of Fig. 8(b)]. As long as the temperature stays above 230 K the anisotropy of the Fe-Tb layer remains smaller than the Co/Pt multilayers. Furthermore, the saturation magnetization, and with it the Zeeman energy of the Fe-Tb alloy film, is much smaller as compared to the Co/Pt multilayers. Therefore, the reversal back into the preferred AFM configuration under the presence of an external field costs less energy for the Fe-Tb layer than for the Co/Pt multilayers. However, below 260 K the situation changes, and the Co/Pt multilayers reverse against the Fe-Tb layer towards remanence [Fig. 8(a), at 90 K]. The reason for this behavior lies in the Fe-Tb layer gaining magnetic anisotropy [inset of Fig. 8(b)] and net magnetization in the lower temperature regime. Thus, the energy barrier for the magnetization reversal consisting of the anisotropy and Zeeman energy becomes larger for the alloy film as compared to the Co/Pt multilayers favoring the observed switching. Finally, at temperatures below 20 K the switching field of the Fe-Tb layer due to the enhanced magnetic anisotropy overcomes the maximum applied magnetic field. This results in the observed positive EB field of the Co/Pt multilayers.

A detailed understanding of the detected AFM interaction between the Fe-Tb alloy film and the Co/Pt multilayers via the formation of an IDW can be derived from the minor loop study at 120 K presented in Fig. 9. Scheme number 1 refers to the saturation configuration in the positive field direction at about 30 kOe. In this state the dominant sublattice moments of Co and Tb aligned parallel and a domain wall owing to the minimization of the AFM exchange energy characterize the interface region. Coming from this point, the reduction of the external field gives rise to the reversal of the Co/Pt multilayer. From the minor loops produced by the field cycling starting from saturation to 2.75 and 4.25 kOe one finds a completely reversible behavior. This indicates that the extinction of the IDW might involve the propagation of a transversal domain wall through the Co/Pt multilayers (see scheme number 2). The antiparallel alignment of the dominant moments, displayed in scheme number 3, illustrates the assumed zero field configuration of the heterostructure, which is free from any domain-wall state. In contrast to the Co/Pt multilayer, the Fe-Tb alloy film shows non-reversibility in the magnetization during the negative field cycling. This can be attributed to the nucleation of lateral domains (see scheme number 4). These domains are highly stable and produce a domain wall at the interface to the corresponding part of the Co/Pt multilayer leading to their partial switching observed when the field is reduced to zero. In a saturation field of

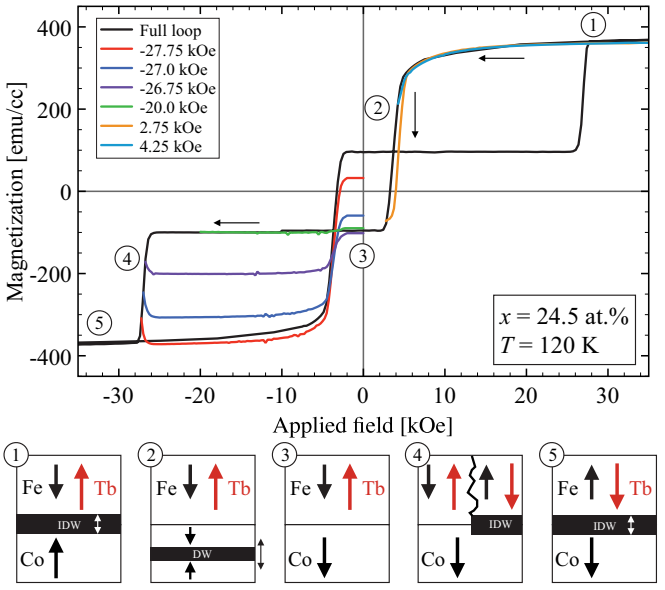

FIG. 9. (Color online) Minor loop reversal taken from out-of-plane SQUID-VSM measurements and a schematic drawing of the assumed domain configuration during the magnetization reversal in $Fe_{75.5}Tb_{24.5}$(20 nm)/[Co(0.4 nm)/Pt(0.8 nm)]$_{10}$ heterostructures.

about −30 kOe the heterostructure reveals the same magnetic configuration as in positive field direction (scheme number 5).

In comparison to heterostructures with a preferred FM coupling, it was found that the interfacial exchange coupling, whether FM or AFM, manifests itself mainly in the sign change of the EB field. Nevertheless, a slight influence of the Fe-Tb layer's composition on the magnitude of the exchange coupling was found and will be discussed in the following section.

3. *The interfacial exchange energy as function of the composition of the Fe-Tb layer*

The EB field represents a measure of the interfacial exchange energy density J_{EB} based on the relation given in Eq. (2). Figures 10(a) and 10(b) summarize J_{EB} and the magnitude of the EB field, respectively, as a function of the Tb content in $Fe_{100-x}Tb_x$/[Co/Pt]$_{10}$ heterostructures at 10 and 120 K. Furthermore, the total EB field is outlined in the inset indicating the sign change from minus to plus at the compensation point when the dominant sublattice moment changes from Fe to Tb. At 10 and 120 K a similar composition dependency becomes apparent, only the total values differ slightly. This is attributed to the increasing effective magnetic anisotropy of the Fe-Tb film towards lower temperatures, which leads to an increasing IDW energy [see Eq. (3)] and a high value for J_{EB}. From 18 to 25 at.% Tb the exchange energy density seems to reach its maximal value. Towards lower and higher amounts of Tb some reduction appears. This behavior cannot be explained by the variation of the effective magnetic anisotropy of the Fe-Tb alloy films [Fig. 4(a)]. Despite its strong relation to the IDW energy and therefore to the interfacial exchange energy [see Eqs. (2) and (3)], the changes in K_{eff} are far too small to explain the observed composition dependency completely. Instead the sperimagnetic spin configuration and in consequence the net magnetization of the Fe-Tb alloy film might play also

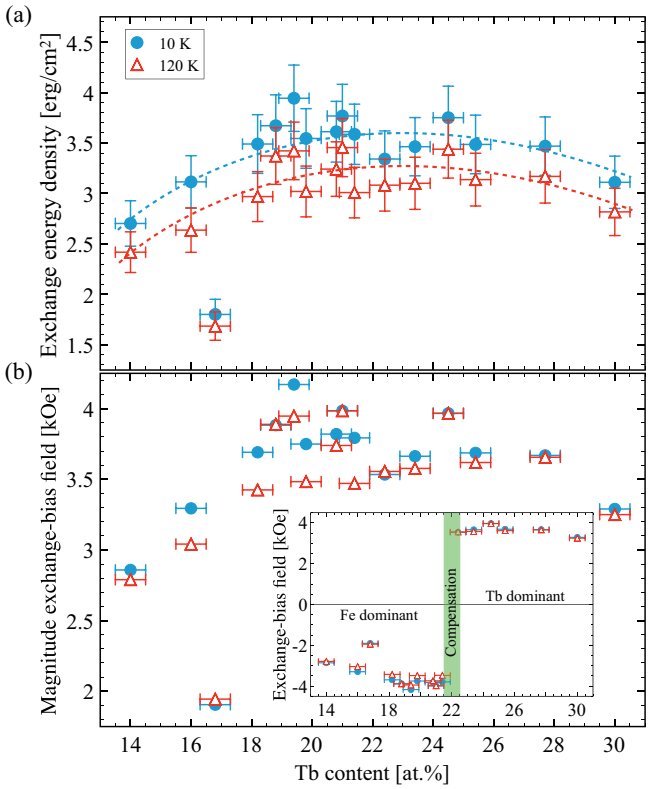

FIG. 10. (Color online) (a) The interfacial exchange energy density and (b) the magnitude of the EB field as a function of the Tb content obtained from $Fe_{100-x}Tb_x$/[Co/Pt]$_{10}$ heterostructures at 10 and 120 K. The dashed curves act as a guide to the eye. The error for the EB field lies within the size of the symbols. And the scattering of data points is most likely related to the interface roughness induced by changes in growth conditions depending on the Tb content of the alloy. Please note that the sign of the EB field changes at a composition of about 22 at.% due to the transition of the dominant magnetic moment from Fe to Tb in the Fe-Tb alloy film as shown in the inset.

an important role. In the recent work of Radu *et al.*[26] as well as Ungureanu *et al.*[27] the authors find that the EB field reaches its maximum at the compensation point, since the compensated sublattices of the FI film hold no frustrated bonds at the interface to the FM layer. With regard to this, the net magnetization has an impact on the exchange energy. However, in our case the influence is rather small, as observed from the composition dependency of the net magnetization shown in Fig. 4(b). While the magnetization increases from almost zero at 21 at.% to 400 emu/cm^3 towards lower and higher amounts of Tb, the exchange energy per unit area decreases only by about 20%.

With regard to the maximum value of $J_{EB} = 3.5$ erg/cm^2 at 10 K the $Fe_{100-x}Tb_x$/[Co/Pt]$_{10}$ heterostructures exhibit by a factor of 10 higher exchange energy densities as other comparable perpendicular exchange-bias systems such as [Co/Pt]/CoO heterostructures.[28]

C. Interfacial exchange coupling depending on the thickness of the FM layer

The magnitude of the EB field in an AFM/FM heterostructure with varying thickness of the FM layer follows typically

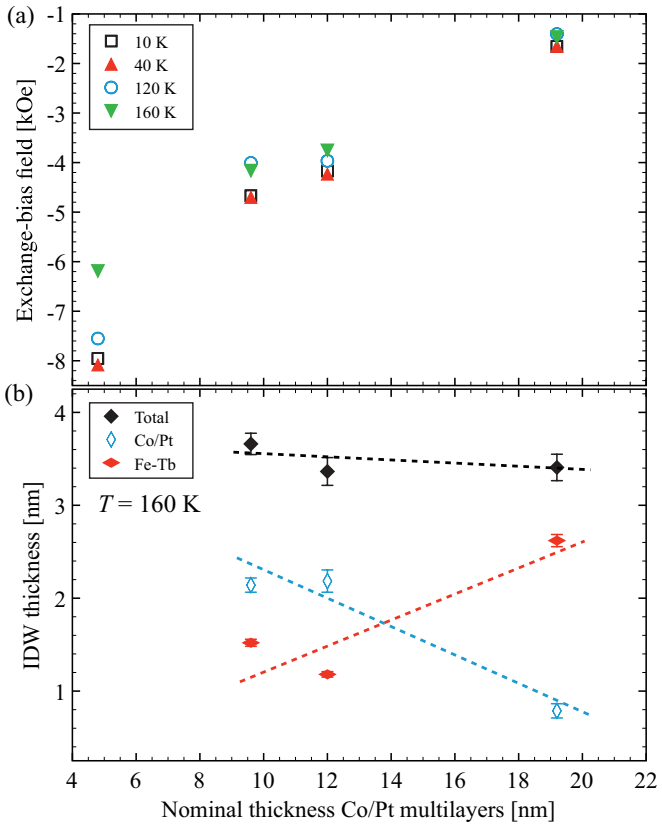

FIG. 11. (Color online) (a) EB field $H_{EB,Co/Pt}$ of the Co/Pt multilayers at 10, 40, 120, and 160 K and (b) the total as well as partial IDW thickness ($t_{IDW} = t_{IDW,Co/Pt} + t_{IDW,Fe\text{-}Tb}$) related to both layers of the heterostructure at 160 K as a function of the nominal thickness of the multilayer stack obtained from SQUID-VSM and XMCD absorption measurements. The dashed lines act as a guide to the eye.

an inverse relation.[22,23] However, this is only valid for high anisotropic AFM materials, which yield a certain amount of uncompensated frozen spins at the interface and disallow the nucleation of a domain wall in the layer itself. In contrast to this, the EB effect in the present FI/FM heterostructure is based on the nucleation of an IDW storing the exchange energy. Therefore one can expect a different dependency of the EB field on the FM layer thickness as compared to the AFM/FM system.

To elucidate this expectation, a series of $Fe_{80.5}Tb_{19.5}$ (20 nm)/[Co(0.4 nm)/Pt(0.8 nm)]$_n$ heterostructures was analyzed with regard to the magnitude of the EB field as a function of the [Co/Pt] bilayer number n by varying n from 4 to 16. The thickness of the Fe-Tb alloy film was held constant at 20 nm.

From the SQUID-VSM and XMCD absorption measurements a nearly linear decrease of the magnitude of the exchange field with increasing thickness of the FM layer was found [Fig. 11(a)]. Except for a small variation in the magnitude this dependence does not change with temperature. An understanding of the linear behavior provides the layer specific thickness of the IDW as a function of the Co/Pt multilayer thickness as presented in Fig. 11(b). While the total thickness of the IDW stays more or less the same, interestingly their location changes with increasing FM layer thickness. This manifests itself in the simultaneous reduction and enhancement of the IDW parts located in the Co/Pt multilayers and in the Fe-Tb layer, respectively. The effective magnetic anisotropy of the Co/Pt multilayers, as obtained from reference samples, changes by about 20% with the number of repetitions from 1.7 Merg/cc for $n = 4$ to 2.2 Merg/cc for $n = 10$. An increase of the number of repetitions to $n = 16$ yield no further anisotropy enhancement. Therefore, the magnetic anisotropy cannot explain the observed shift completely. Another reason might be the gain in magnetic moment towards higher thicknesses increasing the Zeeman energy. In consequence the domain wall moves further into the Fe-Tb layer, until the equilibrium with respect to the magnetic anisotropy energy and exchange energy of the FI material is reached. The Zeeman energy, which follows linearly the magnetic moment, might lead to a corresponding linear shift. Since the Fe-Tb alloy film yields a smaller domain-wall energy density σ_{DW} (3.5 ergs/cm^2) as compared to the Co/Pt multilayers (5.2 ergs/cm^2) due to the different values for the exchange stiffness[19,20] the change in the position of the IDW might cause the linear reduction of the EB field. A change of the location, where the IDW resides, is also known from other rare-earth–transition-metal based heterostructures.[25,29,30]

IV. CONCLUSION

In conclusion, we have investigated the interfacial exchange coupling in perpendicular heterostructures consisting of FI amorphous Fe-Tb alloys and FM Co/Pt multilayers. From element specific hysteresis loops obtained by XMCD absorption measurements, an IDW with a finite size of 3–4 nm was found to exist, when the Co moments are forced to point antiparallel to the Fe moments and parallel to the Tb moments. Due to the exchange interaction between rare-earth and transition-metal moments, this state is energetically inappropriate and the system tries to minimize the energy by nucleating an IDW.

The magnitude of the exchange energy per unit area depends on the net magnetization and effective magnetic anisotropy of the Fe-Tb layer, which was probed by varying the amount of Tb in the film. It was found that with reducing net magnetization towards zero at 21 at.% Tb the exchange energy reaches its maximum. Furthermore, at lower temperatures a small increase was observed, which is attributed to the increasing effective magnetic anisotropy of the Fe-Tb film.

Although in common EB systems an inverse relation between the exchange field and the thickness of the FM layer is expected, the investigated heterostructures show a more linear dependency, which can be attributed to the IDW moving linearly into the Fe-Tb layer with increasing thickness of the Co/Pt multilayers. This leads to a maximum EB field of about 8 kOe in heterostructures with a nominal Co/Pt multilayer thickness of 4.2 nm.

The presented results give rise for a phenomenological understanding of the exchange field characteristic, however an appropriate quantitative model is still missing at the moment. Thus, further investigations are necessary to understand the EB effect in this particular system.

ACKNOWLEDGMENTS

The authors thank HZB for the allocation and financial support of synchrotron radiation beam time. In particular, we thank Torsten Kachel for beamline assistance. Further financial support was provided by the Federal Ministry of Education and Research (BMBF) via the project Nano System Integration Network of Excellence (nanett) and through Landesinnovationspromotion (financed by the European Social Fund and the Free State of Saxony).

[1] W. H. Meiklejohn and C. P. Bean, Phys. Rev. **102**, 1413 (1956).
[2] S. Roy, M. R. Fitzsimmons, S. Park, M. Dorn, O. Petracic, I. V. Roshchin, Z. P. Li, X. Batlle, R. Morales, A. Misra, X. Zhang, K. Chesnel, J. B. Kortright, S. K. Sinha, and I. K. Schuller, Phys. Rev. Lett. **95**, 047201 (2005).
[3] F. Radu and H. Zabel, Springer Tracts Mod. Phys. **227**, 97 (2008).
[4] K. O'Grady, L. Fernandez-Outon, and G. Vallejo-Fernandez, J. Magn. Magn. Mater. **322**, 883 (2010).
[5] W. C. Cain and M. H. Kryder, J. Appl. Phys. **67**, 5722 (1990).
[6] F. Canet, S. Mangin, C. Bellouard, and M. Piecuch, Europhys. Lett. **52**, 594 (2000).
[7] S. Mangin, F. Montaigne, and A. Schuhl, Phys. Rev. B **68**, 140404 (2003).
[8] S. Mangin, T. Hauet, P. Fischer, D. H. Kim, J. B. Kortright, K. Chesnel, E. Arenholz, and E. E. Fullerton, Phys. Rev. B **78**, 024424 (2008).
[9] S. Romer, M. A. Marioni, K. Thorwarth, N. R. Joshi, C. E. Corticelli, H. J. Hug, S. Oezer, M. Parlinska-Wojtan, and H. Rohrmann, Appl. Phys. Lett. **101**, 222404 (2012).
[10] I. Campbell, J. Phys. F **2**, L47 (1972).
[11] Y. Mimura, N. Imamura, and T. Kobayashi, IEEE Trans. Magn. **12**, 779 (1976).
[12] J. M. D. Coey, J. Chappert, J. Rebouillat, and T. Wang, Phys. Rev. Lett. **36**, 1061 (1976).
[13] J. Rebouillat, A. Lienard, J. M. D. Coey, R. Arrese-Boggiano, and J. Chappert, Physica B + C **86-88**, 773 (1977).
[14] K. Handrich and S. Kobe, *Amorphe Ferro- und Ferrimagnetika* (Akademie-Verlag, Berlin, 1980), p. 130.
[15] J. M. D. Coey, J. Appl. Phys. **49**, 1646 (1978).
[16] T. Kobayashi, H. Tsuji, S. Tsunashima and S. Uchiyama, Jpn. J. Appl. Phys. **20**, 2089 (1981).
[17] P. Chaudhari, J. J. Cuomo, and R. J. Gambino, IBM J. Res. Dev. **17**, 66 (1973).
[18] S. Middelhoek, J. Appl. Phys. **34**, 1054 (1963).
[19] S. Hashimoto and Y. Ochiai, J. Magn. Magn. Mater. **88**, 211 (1990).
[20] Y. Mimura, N. Imamura, T. Kobayashi, and A. Okada, J. Appl. Phys. **49**, 1208 (1978).
[21] S. Tsunashima, J. Phys. D: Appl. Phys. **34**, R87 (2001).
[22] J. Nogués and I. K. Schuller, J. Magn. Magn. Mater. **192**, 203 (1999).
[23] R. Stamps, J. Phys. D: Appl. Phys. **33**, R247 (2000).
[24] J. Nogués, C. Leighton, and I. K. Schuller, Phys. Rev. B **61**, 1315 (2000).
[25] T. Hauet, J. A. Borchers, P. Mangin, Y. Henry, and S. Mangin, Phys. Rev. Lett. **96**, 067207 (2006).
[26] F. Radu, R. Abrudan, I. Radu, D. Schmitz, and H. Zabel, Nat. Commun. **3**, 715 (2012).
[27] M. Ungureanu, K. Dumesnil, C. Dufour, N. Gonzalez, F. Wilhelm, A. Smekhova, and A. Rogalev, Phys. Rev. B **82**, 174421 (2010).
[28] S. Maat, K. Takano, S. S. P. Parkin, and E. E. Fullerton, Phys. Rev. Lett. **87**, 087202 (2001).
[29] T. Hauet, S. Mangin, F. Montaigne, J. A. Borchers, and Y. Henry, Appl. Phys. Lett. **91**, 022505 (2007).
[30] M. Watson, T. Hauet, J. A. Borchers, S. Mangin, and E. E. Fullerton, Appl. Phys. Lett. **92**, 202507 (2008).